Identification and Verification of Frequency-Domain Models for XV-15 Tilt-Rotor Aircraft Dynamics in Cruising Flight

Mark B. Tischler*
Aeroflightdynamics Directorate, U.S. Army Aviation Research and Technology Activity
NASA Ames Research Center, Moffett Field, California
and
Joseph G.M. Leung† and Daniel C. Dugan‡
NASA Ames Research Center, Moffett Field, California

Frequency-domain methods are used to extract the *open-loop* dynamics of the XV-15 tilt-rotor aircraft from flight test data for the cruise condition ($V = 170$ knots). The frequency responses are numerically fitted with transfer-function forms to identify equivalent modal characteristics. The associated handling quality parameters meet or exceed level II, category A requirements for fixed-wing military aircraft. Step response matching is used to verify the time-domain fidelity of the derived transfer-function models. The transient responses of the model and aircraft are in close agreement in all cases, except for the normal acceleration response to elevator deflection in cruise. This discrepancy suggests that center-of-rotation corrections in the normal acceleration model are highly sensitive to small changes in flight condition and input form, and should be omitted if a robust model is desired. The utility of the frequency-domain approach for dynamics identification and analysis is clearly demonstrated.

Introduction

THE identification of XV-15 tilt-rotor dynamics (Fig. 1) from flight test data is an extensive ongoing effort to support the development of the next generation of tilt rotors, the Joint Services V/STOL aircraft (JVX). The key concerns of the effort are the documentation of open-loop XV-15 dynamics and the validation of generic tilt-rotor models.[1,2] A frequency-domain-based identification approach was developed and successfully applied for the hover flight condition.[3] Transfer-function models describing the open-loop response characteristics of the XV-15 aircraft were extracted and compared with the simulation characteristics. Reference 3 presents a detailed description of the frequency-domain methodology and the results for the hover flight condition.

As in all identification research, a key concern of this effort is the fidelity of the extracted models for input forms other than those used in the identification process. The flight testing technique of Ref. 3 uses a pilot-generated swept sine wave input to excite the vehicle dynamics. This yields excellent identification of frequency responses and transfer functions for sinusoidal-like inputs. Such information is needed for frequency-domain-based handling quality specifications such as the bandwidth and equivalent systems criteria of the proposed *MIL Handbook* for fixed-wing military aircraft[4] and the proposed Army LHX specification.[5] However, for time-domain specifications[5-7] such as Mil-H-8501, Mil-F-83300, and some elements of the proposed LHX specification, criteria are largely based on responses to step and pulse inputs, so extracted tilt-rotor models must accurately reflect these characteristics as well. The validity of these linearized transfer-function models for large inputs is a question of special concern to the helicopter community.

This paper discusses the identification of transfer-function models for the cruise flight condition (170 knots). This is a good limiting case for comparison with the previous hover results.[3] Frequency-domain results are compared with proposed Mil spec handling qualitities boundaries to illustrate the compliance testing procedure. Time-domain matching is presented to verify the transient response characterisics of the extracted models for the cruise flight condition. These results show the utility of relatively simple transfer-function models for handling qualities and control system applications.

Review of Identification Methodology

This section reviews frequency-domain identification and time-domain verification techniques. The details of the identification approach are extensively discussed in Ref. 3 and are only outlined in the present paper.

Frequency-domain identification is based on the spectral analysis of input and output time histories using fast Fourier transform technique. This analysis produces describing functions which are (complex-valued) linear descriptions of the input-to-output processes. The identification results are presented in Bode plot format: magnitude and phase vs frequency. System bandwidth and effective time delay, important metrics in current handling qualities specifications, can be read directly from these plots. Tabulated frequency response results are fitted with analytical transfer-function forms to extract modal characteristics for handling qualities specifications given in terms of lower-order (equivalent) system models. Also, the transfer-function models can be driven with step inputs to extract familiar time-domain metrics such as rise time, overshoot, and settling time.

The swept sine wave (frequency sweep) input is a good excitation for the frequency-domain identification approach. This excitation results in bounded and reasonable excursions of the aircraft, suitably exciting the important rigid body modes over the entire frequency range of interest (0.2-6.0 rad/s). The input is generated by the pilot in one axis at a time, with minimal regulation of the remaining axes. Starting from a trim condition, the pilot first executes two 20-s-period inputs to ensure good low-frequency identification. Then the frequency of the inputs is slowly increased up to a maximum of about 6 rad/s, yielding a total run length of about 90 s. Repeat runs are executed to allow concatenation

Received March 12, 1985; revision received Feb. 27, 1986.

*Research Scientist. Member AIAA.
†Electronics Engineer.
‡Research Pilot, Aerospace Engineer.

of the 90-s records in the analysis; this technique minimizes the effects of random noise. Two concatenated longitudinal sweeps are shown in Fig. 2.

Once the flight data have been digitized and preprocessed, the input, output, and cross-spectra—$G_{xx}(f)$, $G_{yy}(f)$, and $G_{xy}(f)$, respectively—are calculated using modern Chirp z-transform methods.[3] Specific transfer functions $G(f)$ are obtained from the ratio of the appropriate cross and input auto spectra;

$$G(f) = \frac{G_{xy}(f)}{G_{xx}(f)} \tag{1}$$

and are presented in Bode format. The coherence function γ^2_{xy}, defined as

$$\gamma^2_{xy} = \frac{|G_{xy}|^2}{|G_{xx}|\,|G_{yy}|} \tag{2}$$

is a good indication of the input-to-output linearity and measurement noise. This frequency-dependent parameter may be interpreted as that fraction of the output spectrum estimate which can be accounted for by linear relation with the input spectrum estimate. When the process under investigation is perfectly linear and the spectral estimates are noise free, the coherence function will be unity for all frequencies in the excited input spectrum range. A value of the coherence function less than unity will result from nonlinearities in the system, input/output noise, or cross-coupled control inputs. The magnitude and phase responses are then fitted with analytical transfer-function models to obtain closed-form descriptions of the input-to-output processes. In order to obtain a unique fit of the frequency responses, certain physical restraints on the commonality of the transfer-function denominator factors are imposed. Small decibel deviations in frequency-domain matching can sometimes produce surprisingly large time-domain discrepancies. Therefore the derived transfer-function models are driven with step and doublet-input data from the flight tapes to check their time-domain fidelity.

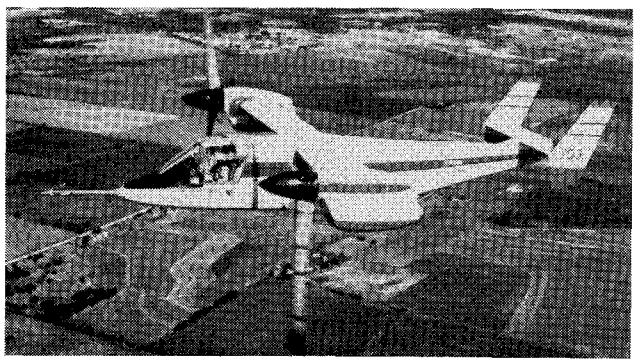

a) cruise configuration

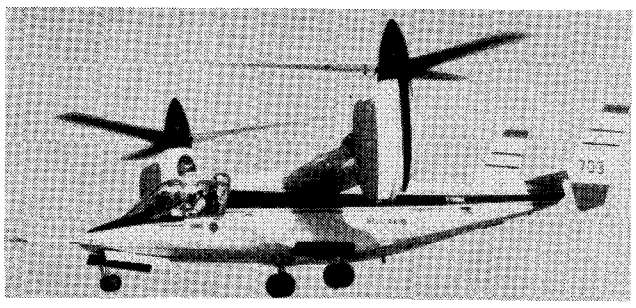

b) hover configuration

Fig. 1 The XV-15 tilt-rotor aircraft.

Dynamics Identification for the Cruise Flight Condition

In this section, the SCAS-OFF (i.e., open-loop) characteristics for the cruise flight condition are considered, with $V = 170$ knots (indicated), nacelle incidence = 0 deg, altitude = 8000 ft. The longitudinal and lateral flight dynamics are fully decoupled in this condition. The primary longitudinal bare-airframe transfer functions of interest are pitch rate and normal acceleration (at the center-of-gravity) responses to elevator deflection, q/δ_e and a_z/δ_e, respectively. The important lateral-directional transfer functions are roll rate response to aileron, p/δ_a, and sideslip (at the center-of-gravity) response to rudder, β_{cg}/δ_r.

Longitudinal Dynamics

The longitudinal stick displacement for two concatenated frequency sweeps were shown in Fig. 2. The sinusoidal stick deflection is regular with a nearly constant amplitude of roughly ±5%. The elevator signal is also regular, with a nearly constant amplitude of 2 deg. These data are typical of the transition-flight and forward-flight condition results. The relative stability of the longitudinal and lateral axes made execution of the frequency sweeps a very rapid and acceptable flight test procedure.

The pitch rate signal (conditioned with a 2.5-Hz low-pass filter for output presentation only) is shown in Fig. 3. The pitch rate excursions are very regular, with a roughly constant peak-to-peak amplitude of 5 deg/s. These oscillations were considered very acceptable to the research pilots and are comparable with those encountered during the hover flight test.[3] The *elevator surface to pitch rate open-loop frequency response* q/δ_e is shown in Figs. 4a-b. The smooth spectral data over the majority of the frequency range are typical of the excellent results obtained from the Chirp z-transform algorithm.[3] Because of the short-period-mode excitation, there is a peak in the pitch rate response at about 2.0 rad/s, with an associated phase lag of 45 deg. At higher frequencies, the magnitude response rolls off at 20 dB/decade and the phase shift approaches −90 deg owing to the K/s pitch rate characteristic and negligible flexibility/servo-lag effects. The drop in the magnitude response and associated positive phase response for frequencies below 0.3 rad/s are due to the phugoid dynamics.

The coherence function shown in Fig. 5 is strong over the frequency range of interest (0.2-6.0 rad/s), as shown. For input frequencies above 7.0 rad/s, the coherence function

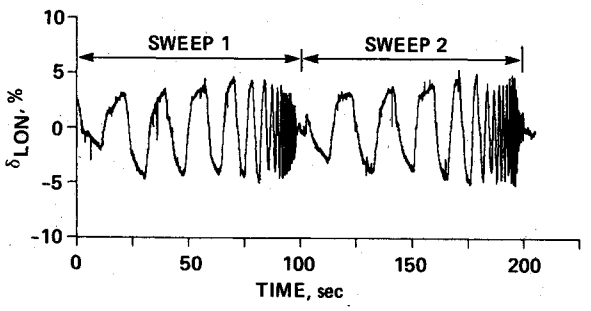

Fig. 2 Two longitudinal stick (δ_{LON}) frequency sweeps in cruise.

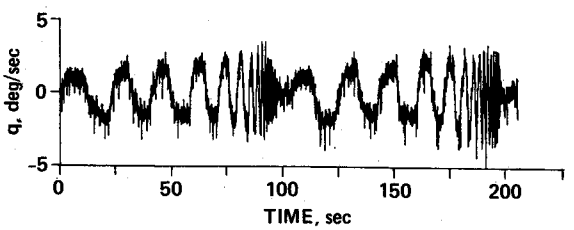

Fig. 3 Pitch rate response q during longitudinal frequency sweeps.

becomes erratic and the transfer-function identification is less accurate. For low-frequency inputs (less than 0.3 rad/s), the pitch rate response decreases, even for the nearly constant input amplitude, owing to the effect of the phugoid dynamics. This results in a decrease of information transfer and an associated drop in the coherence function. This coherence function roll-off is also attributable to atmosphere turbulence effects, which become more important at low frequency where the turbulence spectrum peaks.

Recently proposed military specifications for piloted handling qualities[4] are based on two key frequency-domain parameters: bandwidth ω_{BW} and phase delay τ_p. For a particular stick response transfer function, the bandwidth is defined as that frequency where the phase margin is 45 deg or the gain margin is 6 dB, whichever is lowest. As discussed in Ref. 4, the bandwidth is a measure of the speed of response. A high bandwidth reflects quick response and accurate tracking capability; a low bandwidth suggests sluggish response and pilot-induced oscillation tendencies. The phase delay is a measure of the slope of the phase curve for frequencies near the bandwidth value. A large phase delay (e.g., greater than 100 ms) results in a significant degradation of piloted handling qualities.

For longitudinal control, a key transfer function is pitch attitude response to longitudinal stick, θ/δ_{LON}, which is easily derived from the elevator-to-pitch rate transfer function as

$$\frac{\theta(s)}{\delta_{LON}(s)} = \frac{\delta_e(s)}{\delta_{LON}(s)} \cdot \frac{q(s)}{s\delta_e(s)} \tag{3}$$

where s is the Laplace operator.

The first term in Eq. (3), $\delta_e(s)/\delta_{LON}(s)$, reflects the SCAS-OFF dynamics between the cockpit stick deflection δ_{LON} and the elevator surface deflection δ_e. These dynamics result from surface actuators and mechanical linkages. Frequency response identification of $\delta_e(s)/\delta_{LON}(s)$—and $\delta_a(s)/\delta_{LAT}(s)$ and $\delta_r(s)/\delta_{PED}(s)$—showed that the effective transfer function is a pure gain with an equivalent time delay of less than 10 ms (negligible). In the following discussion, therefore, the results obtained for the response to surface deflection are also converted to effective cockpit control response by simply applying a scale factor.

The Bode plot for pitch attitude response to elevator may be obtained from the pitch rate response by rotating the magnitude curve about the $\omega = 1$ rad/s point by a slope of 20 db/decade. The phase curve is shifted by a constant value of -90 deg. With reference to Fig. 4, the critical bandwidth criterion is the phase margin, which is 45 deg at a frequency of $\omega_{BW_\theta} = 2.5$ rad/s. The effective time delay is negligible, since the phase curve is nearly flat where it is near 180 deg. These bandwidth and time delay values are well within the level II, category A specifications (adequate handling qualities for high-precision tracking tasks) of Ref. 4 and certainly reflect satisfactory characteristics for SCAS failure (open-loop) conditions.

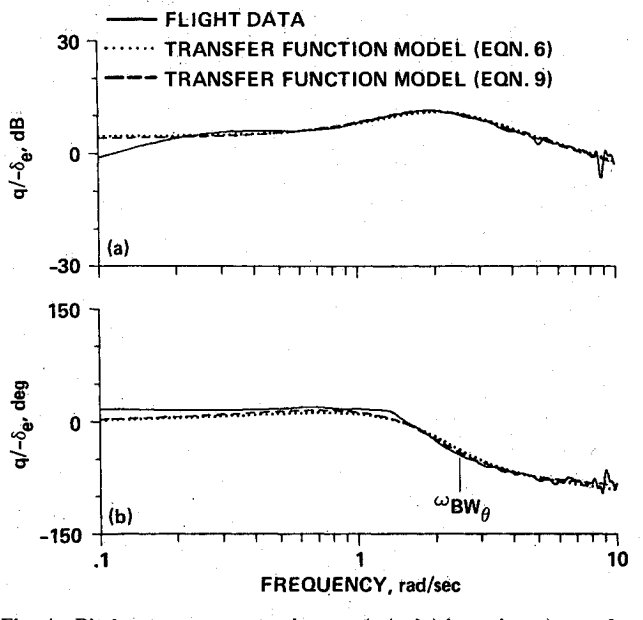

Fig. 4 Pitch rate response to elevator ($q/-\delta_e$) in cruise: a) transfer-function magnitude and b) transfer-function phase.

The Bode plot for *normal acceleration response to elevator*, a_z/δ_e, is shown in Figs. 6a-b. The response is dominated by the classical second-order short-period mode over the majority of the frequency range. The magnitude curve is flat at mid-frequency, indicating a constant normal acceleration response to a step elevator input, with a roll-off in response for frequencies beyond the short-period mode. The fall-off in normal acceleration response for frequencies below 0.3 rad/s is probably due to the dominance of the phugoid dynamics. The phase curve exhibits the classical second-order response, i.e., 0 deg of phase lag at low frequency, 180 deg of phase lag at high frequency, and 90 deg of phase lag at the second-order mode ($\omega \doteq 2.0$ rad/s). This is consistent with the previous pitch rate results. The coherence function for the normal acceleration response shown in Fig. 7 is strong over the frequency range 0.3-10.0 rad/s, with the fall-off at low frequency, again owing to the dominance of phugoid dynamics and turbulence effects. As before, this suggests excellent identification over the entire frequency range of interest.

Longitudinal Transfer-Function Fitting

Analytical transfer-function forms are selected for each degree of freedom based on configuration and flight condition factors. In the hover flight condition, vehicle dynamics are dominated by the hovering cubic and decoupled heave and yaw modes. In wing-borne flight, the conventional longitudinal and lateral quartic equations dominate. Thus transfer-function models which are appropriate for the hover flight condition are not necessarily applicable to forward-flight conditions. Obviously, if a model of high enough order is selected, the parameters can be adjusted to accomodate each flight condition. However, such transfer-function models no longer retain the physical significance of the classical lower-order parameters and are often not unique. Also, higher-order transfer-function models tend to be strongly tuned to the specific inputs which are used in the identification procedures (e.g. a frequency sweep) and can be very poor predictors of other test inputs (e.g., step and pulse inputs) and nearby flight conditions. Therefore, higher-order models are not desirable. In the approach taken in Ref. 3, the minimum-order transfer-function models which can satisfactorily fit the frequency responses are used with the upper limt taken as the physical order of the system.

Examination of the longitudinal frequency responses of Figs. 4a-b and 6a-b shows that the longitudinal dynamics of this flight condition are dominated by the short-period mode ($\omega_{sp} \doteq 2$ rad/s). Therefore we adopt the classical pitch rate and center-of-rotation normal acceleration responses to elevator§:

$$\frac{q(s)}{\delta_e(s)} = \frac{M_{\delta_e}(1/T_{\theta_2})e^{-\tau_\theta s}}{[\zeta_{sp}, \omega_{sp}]} \tag{4}$$

where $q(s)/\delta_e(s)$ is the Laplace-transformed pitch rate response to elevator surface deflection (deg/s/deg—elevator), M_{δ_e} is the elevator pitch sensitivity, $1/T_{\theta_2}$ is the first-order numerator inverse time constant, ζ_{sp} and ω_{sp} are the

§Shorthand notation: $[\zeta, \omega]$ implies $s^2 + 2\zeta\omega s + \omega^2$, where ζ is the damping ratio and ω the undamped natural frequency (rad/s); and $(1/T)$ implies $s + 1/T$ (rad/s).

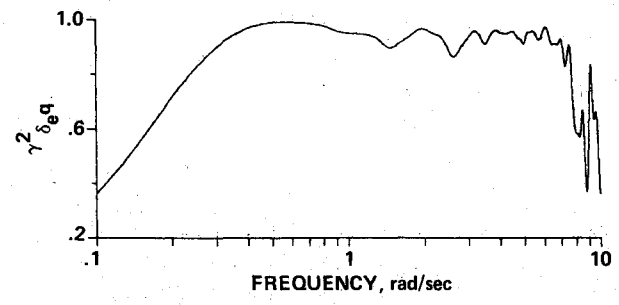

Fig. 5 Coherence function $\gamma^2_{\delta_e q}$ for pitch rate response identification.

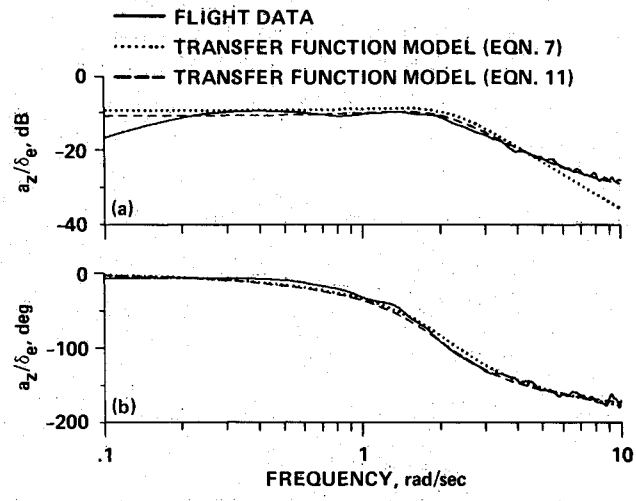

Fig. 6 Vertical-acceleration response to elevator (a_z/δ_e) in cruise: a) transfer-function magnitude and b) transfer-function phase.

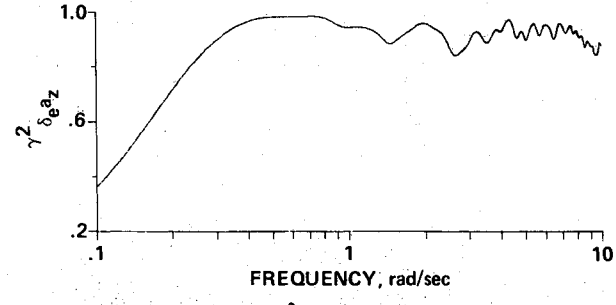

Fig. 7 Coherence function $\gamma^2_{\delta_e a_z}$ for vertical acceleration response identification.

equivalent short-period mode damping and natural frequency, respectively, and τ_θ is the effective time delay; and

$$\frac{a_z(s)}{\delta_e(s)} = \frac{a_{z\delta_e} e^{-\tau_{a_z} s}}{[\zeta_{sp},\ \omega_{sp}]} \tag{5}$$

where $a_z(s)/\delta_e(s)$ is the Laplace-transformed vertical (positive downward) acceleration response at the instantaneous center of rotation to elevator surface deflection (g/deg—elevator), $a_{z\delta_e}$ is the elevator vertical sensitivity and the denominator parameters are identical to those of Eq. (4). The effective time delay for the vertical acceleration response is τ_{a_z}.

We ignore the low-frequency phugoid dynamics, since, as seen from Figs. 4 and 6, these are important only for inputs of the very lowest frequency.

The longitudinal transfer functions of Eqs. (4) and (5) have the same denominator factors, so simultaneous fitting of these responses, while imposing the restriction of commonality of denominator parameters, makes good physical sense. Also, the analyses of Refs. 3 and 8 suggest that such simultaneous fitting techniques are needed to ensure unique and physically meaningful values for the numerator factors. For the longitudinal transfer functions, this avoids the so-called "fixed or free" L_α problem.[4]

The transfer-function parameters of Eqs. (4) and (5) are iteratively varied in order to obtain a best least-squares fit between the equations and the frequency responses of Figs. 4 and 6 over the selected frequency range. For a first-cut model, the center-of-gravity (cg) and longitudinal instantaneous center-of-rotation (ICR) are assumed to be coincident. The iterative fitting procedure is completed using the computer program LONFIT developed by Givan et al.[9] For the present case, the selected range for simultaneous fitting of the pitch rate and normal acceleration responses is 0.3-7 rad/s. In this frequency range, the dynamics are clearly dominated by the short-period mode and the coherence is strong for both transfer functions. Once the short-period damping and natural frequency ζ_{sp} and ω_{sp} are obtained for the simultaneous fit, the high-frequency gain for the normal acceleration response $a_{z\delta_e}$ is varied, holding the damping and frequency constant. This optimizes the a_z fit over the frequency range 0.3-10.0 rad/s, since the coherence function for this measurement remains strong out to higher frequencies. The transfer-function parameters for the pitch rate and normal acceleration responses are finally obtained as

$$\frac{q(s)}{\delta_e(s)} = -\frac{7.727(1.035)e^{-0.016s}}{[0.554,\ 2.179]} \tag{6}$$

$$\frac{a_z(s)}{\delta_e(s)} = \frac{1.597e^{-0.018s}}{[0.554,\ 2.179]} \tag{7}$$

A comparison of these lower-order models with the flight test results is presented in Figs. 4 and 6. The pitch response model matches the data very well over the selected fitting range (0.3-7.0 rad/s for q/δ_e), which shows that the short-period approximation adequately represents the high- and mid-frequency dynamics. For low-input frequencies ($\omega < 0.3$ rad/s), the phugoid mode causes a drop in the pitch response, a characteristic which is not "captured" by the short-period model. The match between the normal acceleration transfer function and the flight data is not nearly as good in the fitting range and shows a noticeable discrepancy in the magnitude response for frequencies greater than 2 rad/s.

Such an error in the mid/high frequency a_z model could arise if the cg and ICR are not coincident. Then the vertical acceleration response at the cg is given approximately by

$$\frac{a_{z_{cg}}}{\delta_e}(s) \doteq \frac{a_{z_{ICR}}}{\delta_e}(s) - \chi_{cg} s \frac{q}{\delta_e}(s) \tag{8}$$

where χ_{cg} is the (unknown) axial location of the center-of-gravity relative to the instantaneous center-of-rotation,

$$\frac{a_{z_{ICR}}}{\delta_e}(s) = \text{acceleration response at the ICR} = \frac{a_z}{\delta_e}(s) \text{ of Eq. (5)}$$

$$\frac{q}{\delta_e}(s) = \text{Eq. (4)}$$

The frequency responses of Figs. 4 and 6 are refit with the models of Eqs. (4) and (8), with χ_{cg} included in the

parameter search. The resulting models are

$$\frac{q(s)}{\delta_e(s)} = \frac{-7.376(0.890)e^{-0.005s}}{[0.536,\ 2.021]} \tag{9}$$

The vertical acceleration response at the center-of-rotation [Eq. (5)] is

$$\frac{a_z(s)}{\delta_e(s)} = \frac{1.166}{[0.536,\ 2.021]} \qquad (\tau_{a_z} = 0) \tag{10}$$

and the location of the cg relative to the ICR is

$$\chi_{cg} = -5.73 \text{ ft} \qquad \text{(cg behind ICR)}$$

The resulting acceleration response at the cg is obtained from Eq. (8):

$$\frac{a_{z_{cg}}(s)}{\delta_e(s)} = \frac{-0.023(-6.699)(7.589)e^{-0.002s}}{[0.536,\ 2.021]} \tag{11}$$

which shows the nonminimum phase (right-half plane) zero that results from the cg located behind the ICR.

The pitch rate model of Eq. (9) is shown in Fig. 4 for comparison with the previous results. Neither the frequency response nor the transfer parameters of the q/δ_e model are significantly altered by including the χ_{cg} degree of freedom. However, the cg acceleration model of Eq. (11) fits the extracted frequency response much closer, as shown in Fig. 6. Thus the noncoincident cg and ICR appear to be a likely source of the discrepancy obtained when the simple model of Eq. (7) is used—rather than the engine rpm response as postulated in the original version of this paper.[10]

Lower-order system parameters are useful in characterizing the vehicle dynamics for comparison with the dynamics of other aircraft. The identified short-period damping and frequency ($\zeta_{sp} = 0.536$ and $\omega_{sp} = 2.021$ rad/s) are consistent with preliminary observations, which are based on the raw Bode plot information. The relatively high degree of damping is a reflection of the small response peak of the pitch rate transfer function. The small effective time delays (in the pitch attitude and normal acceleration transfer fits) indicate that the high-frequency flexibility effects are not important for this flight condition, as noted earlier. The *MIL Handbook* requirements for lower-order equivalent system pitch response are given in terms of the parameters $\omega_{sp}T_{\theta_2}$, ζ_{sp}, and τ_θ. The values of these parameters given in Eq. (9) are well within the level I, category A handling qualities requirements. The bandwidth criteria, which earlier indicated level II SCAS-off handling qualities, are thus more conservative.

Time-domain verification of the longitudinal transfer-function models will be addressed after lateral response models are presented.

Lateral Dynamics

The open-loop Bode plot for *roll rate response to ailerons*, p/δ_a, is shown in Figs. 8a-b. This is a classical first-order system in which aileron inputs produce a constant roll acceleration at high frequency and a constant roll rate at low frequency. The corner frequency is about 1 rad/s, with an associated phase lag of roughly -45 deg, as expected. The dominant time constant is thus roughly 1 s, implying about 2-3 s to reach a steady-state roll rate. The coherence function shown in Fig. 9 is very strong over the frequency range 0.1-9.0 rad/s, indicating excellent identification of the roll rate dynamics.

Specifications for the lateral handling qualities of military aircraft are given in the *MIL Handbook*,[4] based on a lower-order equivalent system model for the roll attitude dynamics (ϕ/δ_{LAT}). When roll-yaw coupling is minor, the specification on the equivalent system roll mode time constant T_r can be interpreted as the reciprocal of the roll response bandwidth ω_{BW_ϕ}. With reference again to Fig. 8b, the bandwidth for roll *attitude* response to *ailerons* is $\omega_{BW_\phi} = 0.9$ rad/s, yielding a dominant time constant of about 1.1 s. Since aileron surface deflection and lateral stick inputs are related by a constant gain, with negligible time delay, the results of Fig. 8b also apply to the pilot's control response. The handling qualities specification of $T_r < 1.4$ s for level I, category A in Ref. 4 is thus satisfied.

Aerodynamic sideslip measurements are obtained from a sideslip indicator located roughly 18 ft ahead of the aircraft cg. The sideslip at the cg β_{cg} is calculated by correcting the measured signal for position error based on yaw rate and airspeed (no flow distortion corrections were made). Also, no corrections are made for sensor dynamics, because these are not felt to be significant within the identification bandwidth.

The Bode plot for *sideslip response* (at the cg) *to rudder inputs*, β_{cg}/δ_r, is shown in Figs. 10a-b. The response is characterized by a lightly damped second-order mode with a frequency of about 1.6 rad/s. High-frequency rudder inputs yield a constant sideslip acceleration, while low-frequency rudder inputs yield a constant sideslip angle corresponding to a steady-state yaw rate. The coherence function for this case, shown in Fig. 11, is strong over the frequency range 0.1-5.0 rad/s, falling off sharply in the high-frequency range. This rapid and relatively low-frequency decline of the coherence function results because the sideslip response falls off at a rate of -40 dB/decade, compared to a roll-off of -20 dB/decade for the other response variables. However, since the yaw mode of interest has a natural frequency of roughly 1.6 rad/s, the falling coherence for frequencies greater than 5 rad/s is not a severe limitation.

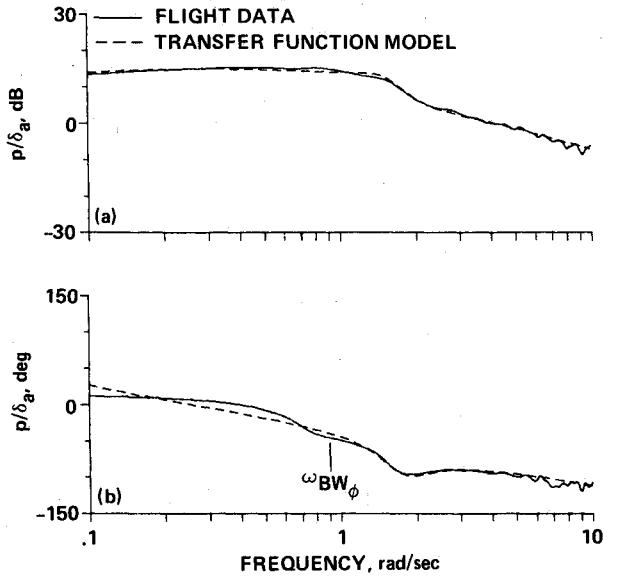

Fig. 8 Roll-rate response to aileron (p/δ_a) in cruise: a) transfer-function magnitude and b) transfer-function phase.

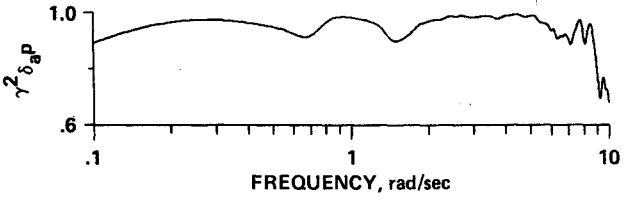

Fig. 9 Coherence function $\gamma^2_{\delta ap}$ for roll rate response identification.

As in the roll axis, handling qualities specifications for the yaw axis response are given in terms of equivalent system models. These are derived in the following section.

Lateral Transfer Function Fitting

Equivalent system fitting using decoupled lateral/directional models have been considered in detail by Bischoff and Palmer.[11] With the *decoupled* model, the responses are fit independently, using a first-order roll rate and a second-order sideslip transfer function. The *coupled* model approach is based on simultaneous fitting of the roll and sideslip responses to obtain the following fourth-order transfer functions:

$$\frac{p(s)}{\delta_a(s)} = \frac{L_{\delta_a} s[\zeta_\phi,\ \omega_\phi]e^{-\tau_\phi s}}{(1/T_s)(1/T_r)[\zeta_d,\ \omega_d]} \tag{12}$$

where $p(s)/\delta_a(s)$ is the Laplace-transformed roll rate response to aileron surface deflection (deg/s/deg—aileron), L_{δ_a} is the aileron roll sensitivity, ζ_ϕ and ω_ϕ are the second-order numerator damping and natural frequency, respectively, $1/T_s$ and $1/T_r$ are the equivalent spiral and roll subsidence modes, ζ_d and ω_d are the equivalent Dutch roll mode damping and natural frequency, respectively, and τ_ϕ is the effective time delay; and

$$\frac{\beta_{cg}(s)}{\delta_r(s)} = \frac{Y_{\delta_r}(1/T_{\beta_1})(1/T_{\beta_2})(1/T_{\beta_3})e^{-\tau_\beta s}}{(1/T_s)(1/T_r)[\zeta_d,\ \omega_d]} \tag{13}$$

where $\beta_{cg}(s)/\delta_r(s)$ is the Laplace-transformed sideslip response to rudder surface deflection (deg/deg—rudder), Y_{δ_r} is the rudder sideslip sensitivity, $1/T_{\beta_1}$, $1/T_{\beta_2}$, and $1/T_{\beta_3}$ are the first-order numerator inverse time constants, and the denominator parameters are identical to those of Eq. (12). The effective time delay for the sideslip response is τ_β. The simultaneous fitting approach is consistent with that used in the longitudinal axis and allows the identification of the ω_ϕ/ω_d "coupling effect" in the roll response [Eq. (12)], which is important in the handling qualities assessment.

The coherence function results of Figs. 9 and 11 show a satisfactory identification of both roll and sideslip responses in the frequency range 0.1-5.0 rad/s. Based on this fitting range, the computer program LATFIT[12] was used to obtain the parameters of Eqs. (12) and (13) simultaneously. Since the coherence for the *roll response* is satisfactory over the entire range of 0.1-10.0 rad/s, this degree of freedom was refit alone, holding the denominator factors constant at the values obtained from the simultaneous solution. This procedure is analogous to that used in the longitudinal case and optimizes the values of the high-frequency gain and numerator parameters in the roll transfer function. The final results for the parameters of Eqs. (12) and (13) are

$$\frac{p(s)}{\delta_a(s)} = \frac{4.486s[0.313,\ 1.887]e^{-0.045s}}{(0.063)(1.090)[0.248,\ 1.581]} \tag{14}$$

$$\frac{\beta_{cg}(s)}{\delta_r(s)} = \frac{-0.051(0.086)(0.818)(47.946)e^{-0.026s}}{(0.063)(1.090)[0.248,\ 1.581]} \tag{15}$$

The lateral/directional transfer-function fits are plotted as dotted lines for comparison with the flight data of Figs. 8 and 10. The matching of the roll response magnitude (see Fig. 8) is excellent over the entire frequency range. Only a slight anomaly in the phase matching is apparent for low-frequency inputs. The agreement between the sideslip fit and the flight data is also excellent (see Fig. 10).

As a result of the simultaneous fitting of the roll and yaw responses, the transfer-function parameters of Eqs. (12) and (13) have clearly retained their physical significance. The inverse roll mode time constant $1/T_r = 1.090$ rad/s is roughly equal to the roll response bandwidth, as expected; both are well within the level I roll response requirements, as mentioned earlier. The equivalent Dutch roll mode is lightly damped, with a natural frequency roughly corresponding to the peak in the sideslip Bode magnitude plot (see Fig. 10a). The small effective time delays for the roll and sideslip responses reflect negligible high-frequency dynamics and are consistent with the previous longitudinal results. The small time delay in the sideslip response also supports the omission of corrections for sideslip sensor dynamics.

The ratio of the natural frequency of the numerator complex zero, ω_ϕ, to that of the denominator complex pole, ω_d, is one measure of roll-yaw coupling in response to aileron inputs. When $\omega_\phi = \omega_d$, the numerator and denominator quadratic factors roughly cancel, and the resulting decoupled roll response is characterized entirely by the roll mode time constant. This case leads to the best handling qualities for a nominal value of the roll mode time constant. As the roll-yaw coupling increases, the numerator and denominator quadratic factors of Eq. (12) no longer cancel and an undesirable oscillatory component of roll rate is generated. With reference to Eq. (14), the near-unity value $\omega_\phi/\omega_d = 1.19$ suggests no such concern for roll-yaw coupling. Therefore a simple, decoupled first-order roll rate model could be adopted for future studies.

Time-Domain Verification of Transfer-Function Models

The transfer function is the minimum realization description of a *linear* input-output process. The transfer-function models developed previously can be used to generate all other frequency- and time-domain information. Therefore a set of verified transfer-function models is a useful output

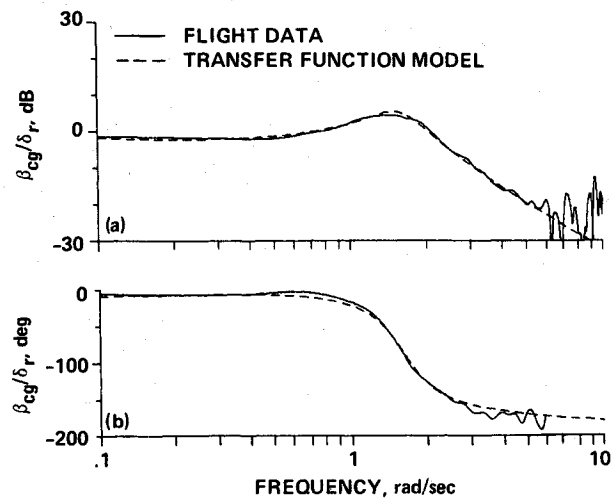

Fig. 10 Sideslip response to rudder (β_{cg}/δ_r) in cruise: a) transfer-function magnitude and b) transfer-function phase.

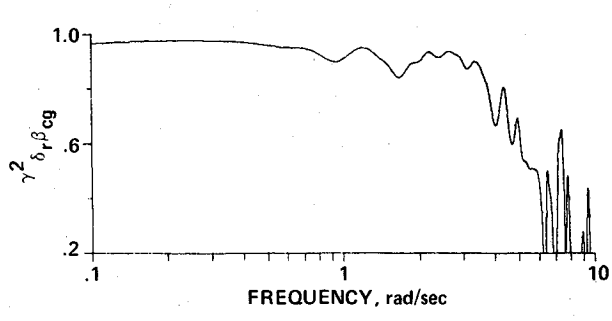

Fig. 11 Coherence function $\gamma^2_{\delta_r\beta_{cg}}$ for sideslip response identification.

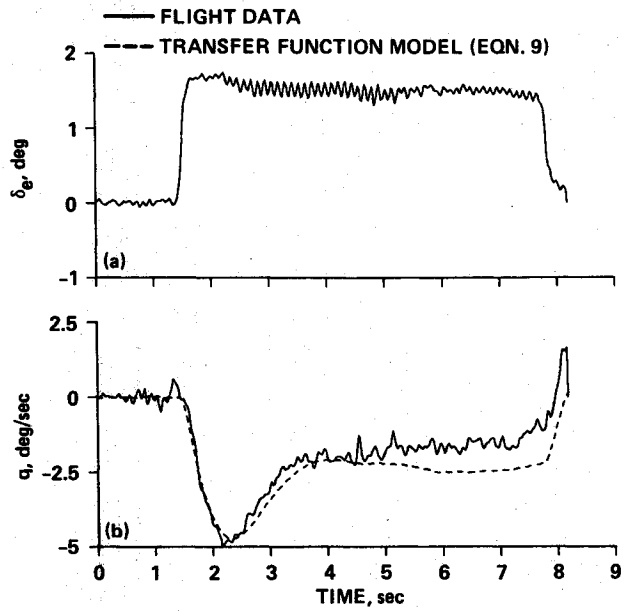

Fig. 12 Comparison of aircraft and transfer-function model responses to a step elevator input in cruise ($h_d = 2800$ ft): a) elevator surface deflection and b) pitch rate response.

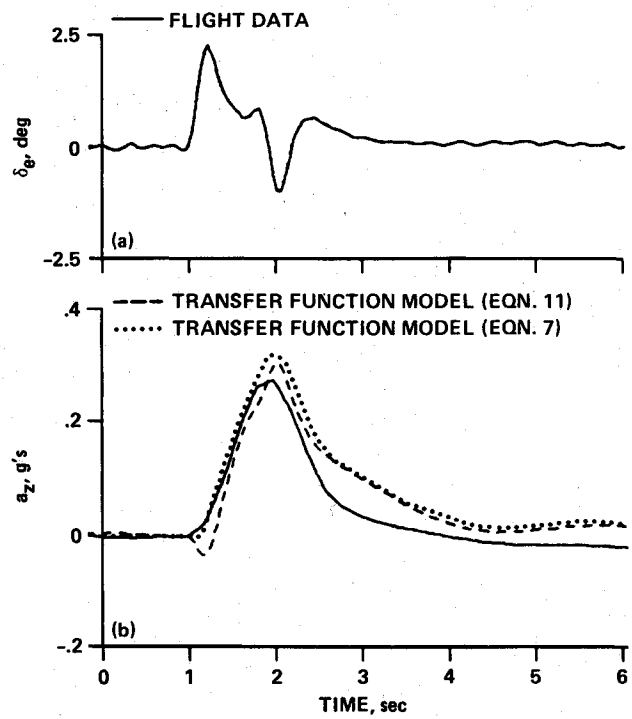

Fig. 13 Comparison of aircraft and transfer-function model responses to a doublet elevator input in cruise ($h_d = 12{,}000$ ft): a) elevator deflection and b) normal (positive downward) acceleration response.

format for the linear identification procedure. However, the adequacy of these linearized transfer-function models for predicting the time-domain dynamics of *nonlinear* systems is at question. For such nonlinear systems, the transfer function is actually a describing function that is strictly valid only for the input amplitudes which were used in the flight test experiment. Also, since identification procedures tend to be tuned to the type of test inputs used (e.g., a sine sweep), their accuracy in predicting responses to other classes of inputs (e.g., steps, doublets) is often uncertain. Lastly, although the mismatches observed in the previous section between the transfer-function fits and the frequency response flight data never exceeded the suggested handling quality specifications, the importance of these discrepancies in predicting time response behavior is still at issue. These questions are addressed in the following section.

For most of the flight tests, frequency sweeps and step inputs were performed consecutively for each flight condition, thus maintaining constant altitude, airspeed, and loading condition. Unfortunately, the open-loop *elevator step response* data for $V = 170$ knots were taken at $H_d = 2800$ ft (density altitude), compared to $H_d = 10{,}000$ ft for the sweeps. Since the indicated airspeed was constant, and therefore also the dynamic pressure, the derived pitch rate model is valid for the lower-altitude step responses. However, the significant difference in true airspeed (about 20 knots) and associated centripetal acceleration ($= U_0 q$) makes an a_z step response comparison invalid for these data (major source of discrepancy in Fig. 20c of Ref. 10). The responses to elevator doublet inputs, obtained from closed-loop (SCAS-ON) tests, for $V = 170$ knots and $H_d = 12{,}000$ ft is used to validate the a_z model, although the aircraft loading condition (and altitude) is still not exactly matched.

The SCAS-OFF (open-loop) pitch rate response to *step elevator deflection* ($H_d = 2800$ ft) is shown in Figs. 12a and b. The elevator input corresponds to about 40% of the maximum control deflection. The comparison between the model response [Eq. (9)] and the flight data is seen to be excellent over the majority of the time history. The slight deviations occurring toward the end of the run are due to the inadequacy of the short-period approximation in modeling the low-frequency (phugoid) dynamics (see Fig. 4). Even so, the short-period approximation clearly gives an excellent characterization of the important initial response dynamics.

The comparison of the ICR-corrected transfer-function model [Eq. (11)] and flight data for the normal acceleration response to an *elevator doublet* input, shown in Fig. 13a, is not as good as it is in the pitch axis. With reference to Fig. 13b, the initial reversal predicted by the model (effect of the χ_{cg} correction) does not occur in the flight response. In fact, if the original center-of-rotation model of Eq. (7) is used, the match with the flight data is much better, as is also shown in Fig. 13b. These results indicate that the $a_{z_{cg}}/\delta_e$ model which includes the center-of-rotation correction [Eq. (8)] is highly tuned to the measured frequency response for sinusoidal inputs (see Fig. 6) and is not robust to small changes in flight condition and input form. The fact that acceleration is a higher-order state derivative compared to the other angular-rate derivatives further exaggerates the sensitivity of this model, especially for the initial (high-frequency) response dynamics. Therefore the lower-order model of Eq. (7) should be used for future handling qualities and control system analyses of this flight condition. This is a good example of the dangers of model overparameterization.

Guidelines are given in the *MIL Handbook*[4] for the maximum allowable mismatch in lower-order system modeling. The discrepancies shown with the simple normal acceleration model [Eq. (7)] in Figs. 6a-b are well within these allowable guidelines, so the identified parameters should be useful indicators of piloted handling qualities. The capability to evaluate directly the effect of model order on response fitting is clearly seen in this example, again representing a unique advantage of the frequency-domain approach for this type of comparison.

The aircraft roll rate response to a step aileron input is shown in Figs. 14a-b. The transfer-function model shown in the dashed line accurately predicts that the response will be predominantly first order, with no overshoot or oscillatory tendency. This corroborates the same conclusion made earlier on the basis of the small ω_ϕ/ω_d ratio. The sideslip response to a step rudder input is shown in Figs. 15a-b with the appropriate corrections for the nose-boom position. The transfer-function model shown in the dashed curve matches

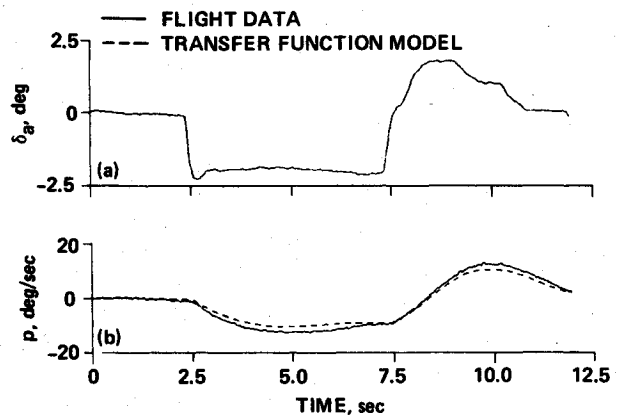

Fig. 14 Comparison of aircraft and transfer-function model responses to a step aileron input in cruise: a) aileron surface deflection and b) roll rate response.

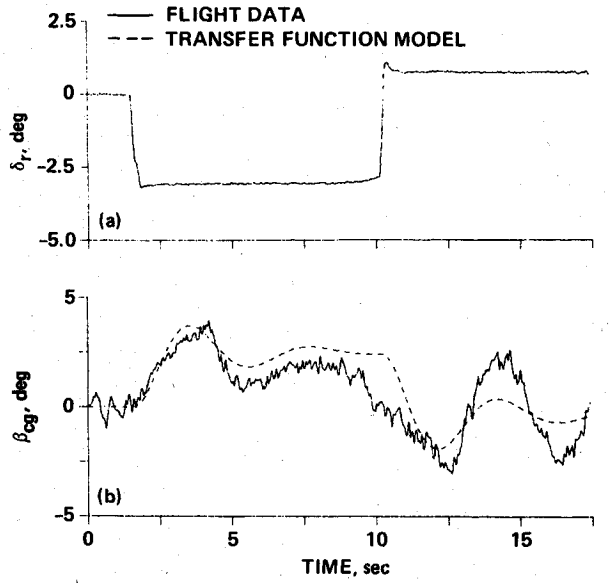

Fig. 15 Comparison of aircraft and transfer-function model responses to a step rudder input in cruise: a) rudder surface deflection and b) sideslip response (at the cg).

the flight data fairly well for the first 10 s. Thereafter the responses diverge, probably owing to a gust encounter or some other aerodynamic interference effect at the sideslip vane during the recovery phase. Once again, the character of the step response is well predicted.

The step response run lengths of roughly 10 s emphasize the high- and mid-frequency ranges, allowing only enough time for about one time constant. Thus the low-frequency mismatches never really have enough time to build up. Clearly, however, the response in the first few seconds is the key concern of the pilot. This is reflected in the mismatch guidelines[4] being most stringent in the mid-frequency range.

This verification study shows that simple transfer-function models extracted from spectral data are accurate in predicting the transient responses to relatively large and varied inputs.

Conclusions

The following are some specific conclusions from this study of the *open-loop* dynamics of the XV-15 tilt-rotor aircraft in the cruise flight condition:

1) The response characteristics are very stable and decoupled. The handling quality parameters meet or exceed proposed level II, category A requirements for fixed-wing military aircraft.

2) Standard lower-order equivalent models adequately match the identified dynamics in all degrees of freedom except for the normal acceleration responses to elevator deflection. While a center-of-rotation correction is needed to accurately fit the a_z/δ_e frequency response data, the resulting higher-order model is not robust to small changes in flight condition and input form.

3) The step responses of the identified transfer functions and the aircraft generally match very well.

The frequency-domain approach has proven to be a relatively simple and accurate means for extracting the bare-airframe dynamics of the XV-15. The utility of the derived lower-order transfer-function models for handling qualities and control system studies has been shown in the frequency and time domains.

References

[1]Ferguson, S.W., "A Mathematical Model for Real-Time Flight Simulation of a Generic Tilt Rotor Aircraft," NAS2-11317, Oct. 1983.

[2]Batra, N.N., Marr, R.L., and Joglekar, M.M., "A Generic Simulation Model for Tilt Rotor Aircraft," Bell-Boeing Report 901-985-002, 1983.

[3]Tischler, M.B., Leung, J.G.M., and Dugan, D.C., "Frequency-Domain Identification of XV-15 Tilt-Rotor Aircraft Dynamics," AIAA Paper 83-2695, Las Vegas, NV, Nov. 1983.

[4]Hoh, R.H., Mitchell, D.G., Ashkenas, I.L., Klein, R.H., Heffley, R.K., and Hodgkinson, J., *Proposed MIL Standard and Handbook—Flying Qualities of Air Vehicles*, Vol. II, AFWAL-TR-82-3081, Flight Dynamics Laboratory, Air Force Wright Aeronautical Laboratories, Wright-Patterson Air Force Base, OH, 1982.

[5]Anon., *Mission-Oriented Flying Qualities Requirements for Military Rotorcraft. Vol. II. Proposed Background Information and User's Guide (BIUG)*, TR-1194-2, Systems Technology, Nov. 1985.

[6]Anon., "Helicopter Flying and Ground Handling Qualities; General Requirements For," MIL-H-8501A, 1961.

[7]Chalk, C.R., Key, D.L., Kroll, Jr., J., Wasserman, R., and Radford, R., "Background Information and User Guide for MIL-F-83300—Military Specification—Flying Qualities of Piloted V/STOL Aircraft," AFFDL-TR-70-88, 1971.

[8]Bischoff, D.E., "The Definition of Short-Period Flying Qualities Characteristics via Equivalent Systems," *Journal of Aircraft*, Vol. 20, June 1983, pp. 494-499.

[9]Givan, M.E., LaManna, W.J., and Hodgkinson, J., *LONFIT User's Guide*," McDonnell Aircraft, St. Louis, MO, Oct. 1978.

[10]Tischler, M.B., Leung, J.G.M., and Dugan, D.C., "Identification and Verification of Frequency-Domain Models for XV-15 Tilt-Rotor Aircraft Dynamics," NASA TM-86009, Aug. 1984.

[11]Bischoff, D.E. and Palmer, R.E., "Investigation of Low Order Lateral Directional Transfer Function Models for Augmented Aircraft," AIAA Paper 82-1610, San Diego, CA, 1982.

[12]Givan, M.E., LaManna, W.J., and Hodgkinson, J., *LATFIT User's Guide*, McDonnell Aircraft, St. Louis, MO, Oct. 1978.